IEEJ Journal of Industry Applications
Vol.6 No.2 pp.117–123 DOI: 10.1541/ieejjia.6.117

Paper

Lens Position Control System Using Limited Pole Placement Method

Yoshiyuki Urakawa[*a)] Senior Member

(Manuscript received May 1, 2016, revised Sep. 22, 2016)

Recently, image sensors for mobile phones have significantly improved, and lens position control is needed for the autofocus actuator of the mobile camera module to realize a robust and precise focus system. The lens position control system is a highly resonant system because the lenses are held by small springs in narrow spaces. In this paper, a digital servo controller for the mobile camera module is discussed. First, continuous control systems are studied for various servo bandwidths with respect to the resonant frequency. Next, three pole assignment methods, 1) multiple poles, 2) a coefficient diagram method, and 3) an optimal controller, are discussed. Third, the limited pole placement method is applied to design a digital controller to suppress the vibration that comes from delay of a system. Finally, a feedforward controller is also investigated to obtain a smooth response for the reference signal. We confirmed that the highly resonant system can be controlled smoothly enough for autofocusing, using the limited pole placement method and the feedforward controller.

Keywords: camera module, autofocus, lens position control, limited pole placement method, feedforward control

1. Introduction

For autofocusing, stepping motors or ultrasonic motors are typically used to position large camera lenses. However, recently, image sensors for mobile phones have greatly improved. Moreover, compact autofocus mechanisms for mobile camera modules are being developed.

Lens actuators for mobile camera modules have almost the same mechanism as the pickups of optical disk drives [1]. The lenses are held by springs, and they are moved by voice coil motors (VCMs). They are highly resonant systems, owing to the fact that the springs in the mobile camera modules are not strong enough to suppress vibrations. How to stably control such resonant systems against a steep phase shift of the resonance is an important problem that needs to be solved.

The servo systems of optical pickups have wide servo bandwidths, and the steep phase shifts of the resonance have a small effect on the stability of the systems [2]–[4]. However, servo systems of mobile camera modules have relatively narrow servo bandwidths and the resonant frequencies are relatively higher. Consequently, the servo controllers need to be adjusted to accommodate the resonance.

In this paper, the digital servo controller of a mobile camera module is designed. First, continuous control systems are studied with three cases of servo bandwidths compared to the resonant frequency. Second, three pole assignment methods are compared: 1) the multiple poles method, 2) the coefficient diagram method (CDM) [5][6], and 3) the optimum controller derived from an algebraic expression [7]. Third, the limited pole placement method [8][9] is applied as a digital redesign method. Thereafter, a feedforward controller is introduced to smoothen the trajectory, using the Pole-Zero Cancellation Method [10]. A lens position control system for highly resonant systems can therefore be designed using the limited pole placement method and feedforward controller.

a) Correspondence to: Yoshiyuki Urakawa. E-mail: Yoshiyuki.Urakawa@jp.sony.com
* Sony Semiconductor Solutions corporation
1-14-1, Asahi-cho, Atsugi, Kanagawa 243-0014, Japan

2. Controllers for Highly Resonant System

Continuous controllers relating to three cases of servo bandwidths are designed. The control system is shown in Fig. 1. The plant is a second-order system with a resonant frequency of 1.0 rad/s. It is controlled by the high gain servo controller [11] (also called complex PIL controller [12], expanded PID controller [5]), which can have not only real zeros but complex zeros as well.

Three sets of control parameters which assign multiple poles at −0.5 rad/s, −1.0 rad/s, and −2.0 rad/s, respectively, are calculated using the direct method. Table 1 shows the parameters, and Fig. 2 shows the open loop frequency characteristics.

Figure 2a) shows the open loop frequency characteristics of multiple poles at −0.5 rad/s with frequencies which are lower than the resonant frequency. The controller has an unstable zero. The position controller for an antenna of a satellite is also known to have an unstable zero [5].

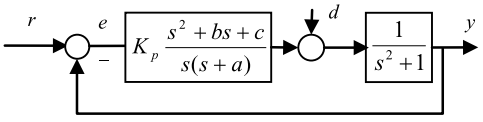

Fig. 1. Control system of resonant plant

Table 1. Control Parameters of multiple poles

	−0.5 [rad/s]	−1.0 [rad/s]	−2.0 [rad/s]
K_p	0.5	5	23
a	2	4	8
b	−3	0	1.044
c	0.125	0.2	0.696

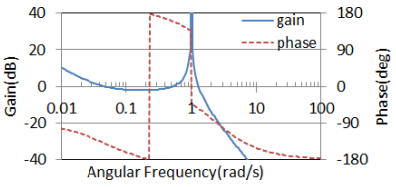

a) Poles of closed loop are assigned at −0.5 [rad/s]

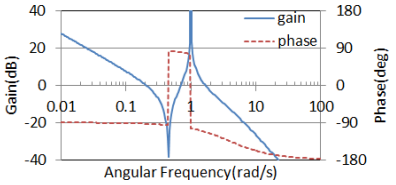

b) Poles of closed loop are assigned at −1.0 [rad/s]

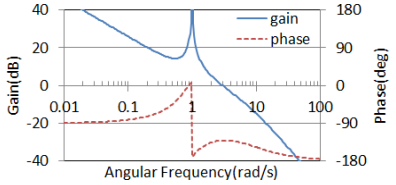

c) Poles of closed loop are assigned at −2.0 [rad/s]

Fig. 2. Resonant frequency and servo bandwidth

Figure 2b) shows the case of multiple poles at −1.0 rad/s with frequencies which are the same as the resonant frequency. The controller has zeros on the imaginary axis, and thus, the phase leads steeply. It is called a "Zero PID Controller" [5], because the proportional gain of the controller equals to zero. It has the largest phase margin.

Figure 2c) shows the case of multiple poles at −2.0 rad/s with frequencies that are higher than the resonant frequency. The resonance is suppressed by the control loop because of the high gain.

In the case of optical pickups, the zero-cross frequency is around ten times higher than the resonant frequency; therefore, the effect of the resonance is sufficiently suppressed. In the case of the AF actuator of mobile phones, the resonant frequency is 70–80 Hz, and the servo bandwidth is only a little wider than 100 Hz. We are therefore dealing with either the case of Fig. 2b) or Fig. 2c).

3. Pole Assignment of Lens Position System

In the previous section, multiple poles are assigned simultaneously; although, there may be other good assignment methods. In this section, three pole assignment methods are discussed; 1) the multiple poles method, 2) CDM [5][6], and 3) the optimum controller derived from an algebraic expression [7]. Step responses for disturbance, open loop frequency characteristics and complementary sensitivity functions are compared. The step response for disturbance, from d to y in Fig. 1, is used to evaluate the pole assignment because it is more suitable than the step response for reference, from r to y in Fig. 1. The reason being that the step response for disturbance is determined only by pole positions, whereas the reference response can be altered by the positions of zeros, using the feedforward controller as discussed in section 5.

3.1 Multiple Poles Step responses of multiple poles at −0.5 rad/s, −1.0 rad/s, and −2.0 rad/s are shown in Fig. 3a). The positions of the lenses are settled without overshoot. The open loop frequency characteristics are shown in Fig. 3b).

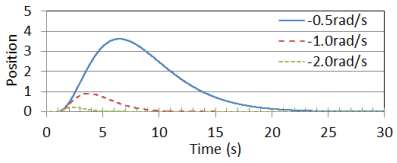

a) Step disturbance response

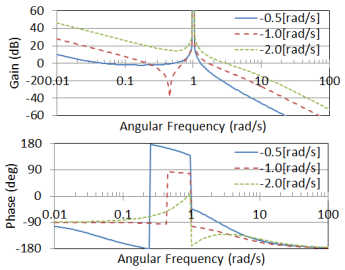

b) Open loop frequency characteristics

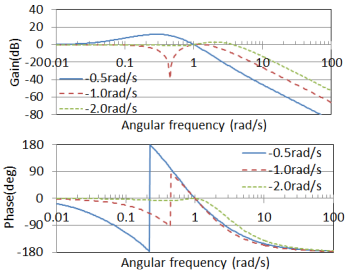

c) Complementary sensitivity functions

Fig. 3. Characteristics of multiple pole system

The case of −1.0 rad/s has the largest gain margin and the largest phase margin. The complementary sensitivity functions are shown in Fig. 3c). The H∞ norm of the −1.0 rad/s case is the smallest.

3.2 CDM CDM is an algebraic control parameter design method, using a logarithmic diagram, on which the coefficients of the characteristic polynomial are plotted. This is achieved in order to balance the stability and the robustness of the system. When the characteristic polynomial is Eq. (1), the stability index γ_i and the equivalent time constant τ are expressed as Eqs. (2) and (3), respectively.

$$P(s) = a_n s^n + \cdots a_1 s + a_0 = \sum_{i=0}^{n} a_i s^i \cdots\cdots\cdots\cdots (1)$$

$$\gamma_i = a_i^2/(a_{i+1}a_{i-1}), \quad i = 1 \sim n-1 \cdots\cdots\cdots\cdots\cdots (2)$$

$$\tau = a_1/a_0 \cdots\cdots\cdots\cdots\cdots\cdots\cdots\cdots\cdots\cdots (3)$$

The stability indices, $\gamma_n = \ldots = \gamma_2 = 2$, $\gamma_1 = 2.5$, are recommended. Typically, the number of parameters is not enough to satisfy all the recommended indices, and it is necessary to tune the parameters, using the diagram, in order to balance the stability and robustness of the system. However, in the example of Fig. 1, P(s) is a polynomial of degree four and the number of parameters is also four. We can therefore calculate the parameters that satisfy the recommended indices completely, for each equivalent time constant τ. The equivalent time constants are set as $\tau = 7.3$ s, $\tau = 3.0$ s, and $\tau = 1.6$ s, which have almost the same zero cross frequency as the multiple poles at −0.5 rad/s, −1.0 rad/s, and −2.0 rad/s, respectively. Table 2 shows the calculated parameters. The step responses are shown in Fig. 4a). The responses converge to zero faster than the responses of the multiple poles shown in

Table 2. Control Parameters of CDM

	τ = 7.3 [s]	τ = 3.0 [s]	τ = 1.6 [s]
K_p	−0.0617	4.556	18.531
a	1.37	3.333	6.25
b	16.984	0.285	1.31
c	−0.713	0.339	1.03

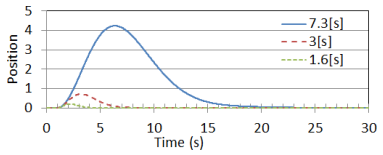

a) Step disturbance response

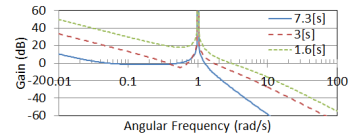

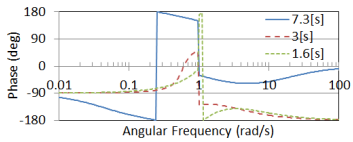

b) Open loop frequency characteristics

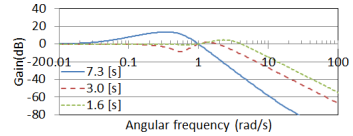

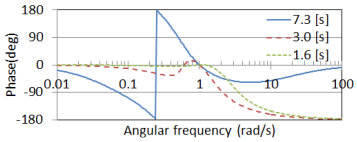

c) Complementary sensitivity functions

Fig. 4. Characteristics of coefficient diagram method

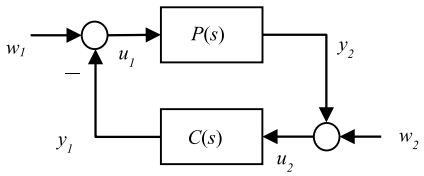

Fig. 5. Control system for optimal transient stabilization

Fig. 3a). The open loop frequency characteristics are shown in Fig. 4b). In the case of τ = 3.0 s, the phase margin is large. The complementary sensitivity functions are shown in Fig. 4c). The H∞ norm of the case τ = 3.0 s, is the smallest of the three, although a little larger than the multiple poles at −1.0 rad/s.

3.3 Optimal Controller Reference [7] shows a method for deriving an optimal controller from an algebraic expression of the plant, which seems suitable for this example. Figure 5 shows the control system. A characteristic polynomial of the optimal controller is decided on using the following algorithm, which makes the evaluation function, Eq. (5), smallest when the plant is expressed as Eq. (4).

$$P(s) = \frac{b(s)}{a(s)} = \frac{b_0 s^n + b_1 s^{n-1} + \cdots + b_n}{a_0 s^n + a_1 s^{n-1} + \cdots + a_n} \cdots\cdots\cdots (4)$$

$$J_{\rho,\mu} = (\|y_1(t)\|_2^2 + \rho^2 \|y_2(t)\|_2^2)|_{w_1(t)=\mu\delta(t),w_2(t)=0}$$

Table 3. Control Parameters of optimum controllers

	$\rho = \mu$ = 0.6	$\rho = \mu$ = 1.5	$\rho = \mu$ = 5.3
K_p	1.665	4.211	18.574
a	1.153	2.534	5.929
b	0.115	0.483	1.402
c	0.817	0.772	1.566

$$+(\|y_1(t)\|_2^2 + \rho^2 \|y_2(t)\|_2^2)|_{w_1(t)=0,w_2(t)=\delta(t)} \cdots\cdots (5)$$

Step 1. Calculate $d_\rho(s)$ using Eq. (6)

$$a(-s)a(s) + \rho^2 b(-s)b(s) = d_\rho(-s)d_\rho(s) \cdots\cdots\cdots (6)$$

Step 2. Calculate $d_\mu(s)$ using Eq. (7)

$$a(-s)a(s) + \mu^2 b(-s)b(s) = d_\mu(-s)d_\mu(s) \cdots\cdots\cdots (7)$$

Step 3. The characteristic polynomial is $d_\rho(s)d_\mu(s)$.

If the plant is expressed as Eq. (8), the characteristic polynomial is decided as follows. First, $d_\rho(s)$ is evaluated, and yield Eq. (10) from Eq. (9). Moreover, $d_\mu(s)$ is evaluated, and yield Eq. (12) from Eq. (11).

$$P(s) = \frac{b(s)}{a(s)} = \frac{1}{s^2+1} \cdots\cdots\cdots (8)$$

$$a(-s)a(s) + \rho^2 b(-s)b(s) = (s^2+1)^2 + \rho^2 = d_\rho(-s)d_\rho(s) \cdots\cdots\cdots (9)$$

$$d_\rho(s) = s^2 + \sqrt{2\sqrt{1+\rho^2} - 2}\, s + \sqrt{1+\rho^2} \cdots\cdots (10)$$

$$a(-s)a(s) + \mu^2 b(-s)b(s) = (s^2+1)^2 + \mu^2 = d_\mu(-s)d_\mu(s) \cdots\cdots\cdots (11)$$

$$d_\mu(s) = s^2 + \sqrt{2\sqrt{1+\mu^2} - 2}\, s + \sqrt{1+\mu^2} \cdots\cdots (12)$$

The optimal characteristic polynomial is then given as $d_\rho(s)d_\mu(s)$, and the parameters for the controller in Fig. 1 can be calculated using the direct method. Table 3 shows the parameters in the cases of $\rho = \mu$ = 0.6, $\rho = \mu$ = 1.5 and $\rho = \mu$ = 5.3, which have almost the same zero cross frequency as the multiple poles at −0.5 rad/s, −1.0 rad/s, and −2.0 rad/s, respectively.

The step responses are shown in Fig. 6a). They appear oscillatory even though the peak values are small. It seems to come from the evaluation function, Eq. (5), which uses only the position, y_2, and does not use the velocity. The open loop frequency characteristics are shown in Fig. 6b). The phase margins are small. The complementary sensitivity functions are shown in Fig. 6c), and the H∞ norms are almost the same for all three cases.

According to the above results, the pole assignment with CDM seems suitable for a controller of lens actuators for mobile phones, because of its fast convergence without oscillation.

4. Application of Limited Pole Placement Method

Next, a digital controller is designed for real-world application using the limited pole placement method [8][9]. Figure 7 shows a schematic drawing of a lens positioning system, and

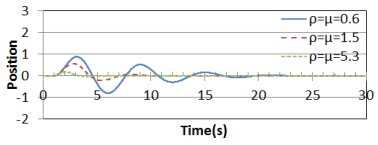

a) Step disturbance response

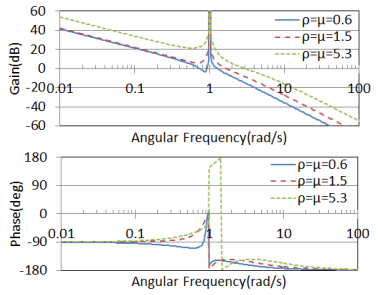

b) Open loop frequency characteristics

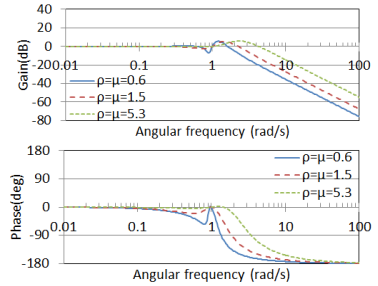

c) Complementary sensitivity functions

Fig. 6. Characteristics of optimal transient stabilization

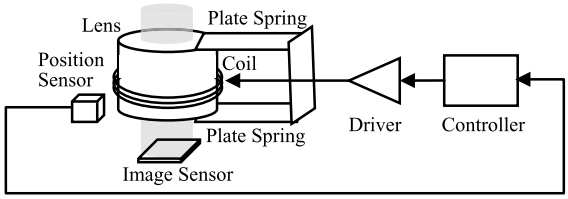

Fig. 7. Schematic drawing of lens position control system

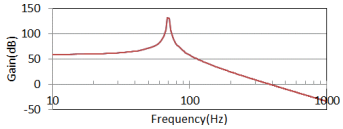

a) gain

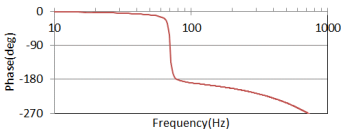

b) phase

Fig. 8. Open loop frequency characteristics of the plant

Fig. 8 shows the frequency characteristics of the plant. The resonant frequency of the plant is 70 Hz. Figure 9 is a block diagram of this sample. The sampling frequency is 10 kHz, and the system has 3 sampling time delays. The digital control parameters: K_{pz}, a_z, b_z, and c_z, which enable the CDM pole assignment, are calculated using the limited pole placement method.

The limited pole placement method is a method used to calculate the parameters of a digital controller. If a digital delay, i.e., a calculation delay, exists, it increases the order of

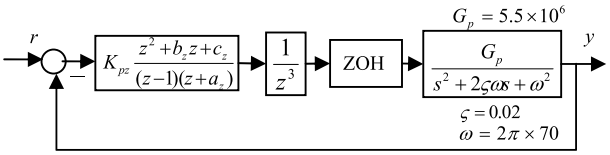

Fig. 9. Block diagram of lens position control system (discrete system)

the control system. Consequently, the controller is not able to assign all of the poles of the system, because it does not have a sufficient number of parameters. The poles shift to oscillatory positions because the delay creates a phase lag. With the limited pole placement method, the poles are divided into two groups: "assigned poles" and "determined poles." The "assigned poles", having as many poles as there are control parameters, are positioned exactly. The other group, "determined poles", has their positions calculated using control parameters. The exactly positioned "assigned poles" makes the response less oscillatory, whilst the "determined poles" indicate the effect of the delay with their positions. For example, if one of the "determined poles" is outside the unit circle, this indicates that the delay makes the system unstable.

The discrete plant that is derived from the plant and the zero order hold is expressed as Eq. (13).

$$P(z) = \frac{n_1 z + n_0}{z^2 + d_1 z + d_0} \quad \cdots\cdots (13)$$

where,

$$n_1 = 2.747945 \times 10^{-2}$$
$$n_0 = 2.746334 \times 10^{-2}$$
$$p_1 = -1.996310$$
$$p_0 = 0.998242$$

The "fixed part", which comes from the discrete plant, the delay, and the fixed polynomial of the controller, i.e., z−1 of the integrator, is expressed as Eq. (14). The "parameter part", which comes from the polynomials with control parameters, is expressed as Eq. (15).

$$\frac{n(z)}{d(z)} = \frac{1}{z-1}\frac{1}{z^3}\frac{n_1 z + n_0}{z^2 + d_1 z + d_0} = \frac{b_1 z + b_0}{z^6 + a_5 z^5 + a_4 z^4 + a_3 z^3} \quad \cdots\cdots (14)$$

$$\frac{\beta(z)}{\alpha(z)} = K_p \frac{z^2 + bz + c}{z + a} = \frac{\beta_2 z^2 + \beta_1 z + \beta_0}{\alpha_1 z + \alpha_0} \quad \cdots\cdots (15)$$

The order of the characteristic polynomial, n_γ, is 7. The number of parameters is 4, and the number of "assigned poles", n_p, is also 4. Moreover, the number of "determined poles", $n_q = n_\gamma - n_p$, is 3. The four "assigned poles" are expressed as p_1, p_2, p_3, and p_4, and the three "determined poles" are expressed as q_1, q_2, and q_3. The characteristic polynomial, $\gamma(z)$, is then expressed as Eq. (16).

$$\gamma(z) = (z-p_1)(z-p_2)(z-p_3)(z-p_4)(z-q_1)(z-q_2)(z-q_3) = (z^4 + P_3 z^3 + P_2 z^2 + P_1 z + P_0)(z^3 + Q_2 z^2 + Q_1 z + Q_0) \quad \cdots\cdots (16)$$

Using Eqs. (14), (15), and (16), the Diophantine equation

Table 4. Control parameters of limited pole placement method

τ [s]	0.006	0.004	0.003	0.0025	0.0024
K_{pz}	0.2241	0.6739	3.0585	3.7698	4.8572
a_z	−0.7970	−0.6208	0.0982	0.2982	0.6001
b_z	−1.9822	−1.9565	−1.9244	−1.9209	−1.9170
c_z	0.9830	0.9579	0.9274	0.9241	0.9205
q_1	0.0626	0.0508	−0.0199	−0.1917	−0.2552
q_2	±0.1982j	±0.3071j	±0.4278j	±0.4877j	±0.4577j
q_3	−0.1653	−0.2349	−0.3275	−0.5197	−0.6782

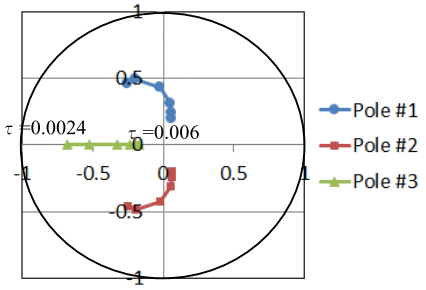

Fig. 10. Position of determined poles

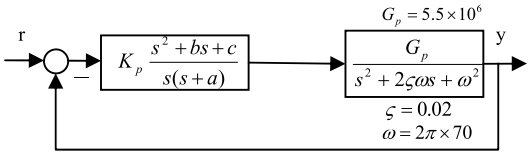

Fig. 11. Block diagram of lens position control system (continuous system)

for the pole placement is expressed as $\theta^T E = \psi^T$ in matrix form, where θ^T, E, and ψ^T are represented by Eqs. (17), (18), and (19), respectively.

$$\theta^T = \begin{bmatrix} \alpha_0 & \alpha_1 & \beta_0 & \beta_1 & \beta_2 & Q_0 & Q_1 & Q_2 \end{bmatrix} \cdots\cdots\cdots (17)$$

$$\psi^T = \begin{bmatrix} 0 & 0 & 0 & P_0 & P_1 & P_2 & P_3 & 1 \end{bmatrix} \cdots\cdots (18)$$

$$E = \begin{bmatrix} 0 & 0 & 0 & a_3 & a_4 & a_5 & 1 & 0 \\ 0 & 0 & 0 & 0 & a_3 & a_4 & a_5 & 1 \\ b_0 & b_1 & b_2 & 0 & 0 & 0 & 0 & 0 \\ 0 & b_0 & b_1 & b_2 & 0 & 0 & 0 & 0 \\ 0 & 0 & b_0 & b_1 & b_2 & 0 & 0 & 0 \\ -P_0 & -P_1 & -P_2 & -P_3 & -1 & 0 & 0 & 0 \\ 0 & -P_0 & -P_1 & -P_2 & -P_3 & -1 & 0 & 0 \\ 0 & 0 & -P_0 & -P_1 & -P_2 & -P_3 & -1 & 0 \end{bmatrix} \cdots\cdots (19)$$

The parameters and the "determined poles" are derived from the equation: $\theta^T = \psi^T E^{-1}$.

Table 4 shows the parameters of the digital controller. Pole assignments are decided upon using CDM in the continuous system. The poles are translated to the digital system using $z = e^{st}$. The parameters and the "determined poles" are calculated using Eqs. (17), (18), and (19). Figure 10 shows the positions of the "determined poles" on the z-plane. Pole #3 moves in the negative direction from τ = 0.006 s, and approaches z = −1 when τ = 0.0024 s. If τ is smaller than 0.0024 s, pole #3 moves outside the unit circle, thus signifying that the system has become unstable. In other words, τ = 0.0024 s is the boundary of the stable system.

Next, Tustin transform, which is the most popular method

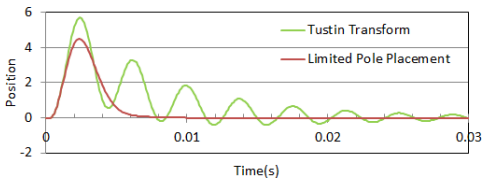

Fig. 12. Step response for disturbance

of digital redesign, is compared to the limited pole placement method. A continuous controller is designed for the control system in Fig. 11, with CDM and τ = 0.003 s. The parameter set comprising of K_p = 0.9643, a = 3315.74, b = 752.0, and c = 290964, is calculated. The controller with this parameter set is then transformed to a digital controller by the Tustin transform. The parameter set of the digital controller is K_{pz} = 0.8589, a_z = −0.7156, b_z = −1.9255, c_z = 0.9269. The step response of this controller is shown in Fig. 12. The step response of the parameter, set by the limited pole placement method in Table 4 (τ = 0.003 s), is also drawn for comparison. It is evident that the parameter set of the limited pole placement method is less oscillatory.

The Tustin transform is known to have a large discretization error around the Nyquist frequency. Consequently, the oscillatory response may include the effects of this discretization error. However, the controller operates at a much lower frequency than the Nyquist frequency, 5 kHz (= 31415.9 rad/s). For example, a pole of this controller is at −3315.74 rad/s, and the pole of the controller is transformed to 0.7156 on the z-plane by the Tustin transform. The correct position of the pole by $z = e^{st}$ transform, is 0.7178, and the discretization error is almost 0.3%. The oscillatory response in this example seems to originate mainly from the delay. Moreover, the limited pole placement method is an effective technique for suppressing the oscillation that comes from the delay.

5. Feedforward Controller

The closed frequency characteristics of the parameter set, τ = 0.006 s in Table 4, of the limited pole placement method are shown in Fig. 13. The gain characteristic, represented by Fig. 13a), has a slightly notched curve at 50 Hz. This is because the resonant frequency of the plant is close to the zero cross frequency of the system. The phase of the open loop frequency characteristics needs to be lead steeply at a little lower frequency than the resonant frequency to make the system stable. This steep phase shift of the open loop frequency characteristics creates the notched characteristic of the closed frequency characteristics in Fig. 13. However, this notched characteristic seems to create the oscillatory step response for the reference.

Figure 14 shows the simulated data. It shows that the lens moves in an oscillatory manner that is undesirable for an AF actuator. The feedforward controller is therefore introduced to smoothen the response using the Pole-Zero Cancellation Method [10].

Figure 15 shows the control system with the feedforward controller. The reference transfer function is expressed as Eq. (20).

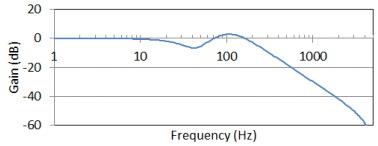

a) gain

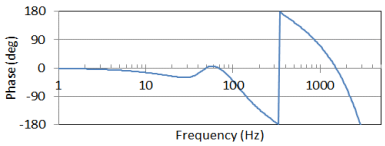

b) phase

Fig. 13. Closed loop frequency characteristics

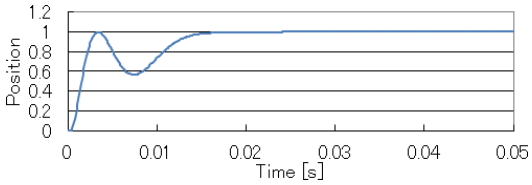

Fig. 14. Reference step response

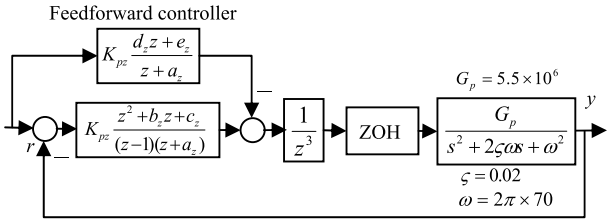

Fig. 15. Block diagram of control system (with feedforward controller)

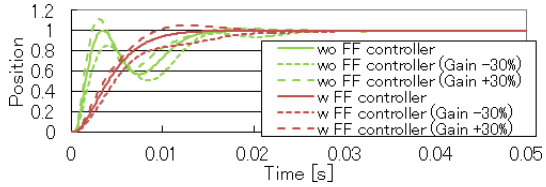

Fig. 16. Step response for reference (with and without feedforward controller)

$$G(z) = \frac{\left(K_{pz}\dfrac{z^2+b_z z+c_z}{(z-1)(z+a_z)} - K_{pz}\dfrac{d_z z+e_z}{z+a_z}\right)\dfrac{1}{z^3}\dfrac{n_1 z+n_0}{z^2+d_1 z+d_0}}{1+K_{pz}\dfrac{z^2+b_z z+c_z}{(z-1)(z+a_z)}\dfrac{1}{z^3}\dfrac{n_1 z+n_0}{z^2+d_1 z+d_0}}$$
$$= \frac{K_{pz}((1-d_z)z^2+(b_z+d_z-e_z)z+(c_z+e_z))(n_1 z+n_0)}{z^3(z-1)(z+a_z)(z^2+d_1 z+d_0)+K_{pz}(z^2+b_z z+c_z)(n_1 z+n_0)} \quad \cdots\cdots (20)$$

The parameters, d_z and e_z, assign the zeros of the reference transfer function. When the zeros are assigned at p_{z1} and p_{z2}, d_z and e_z, are evaluated, yielding Eqs. (21) and (22), respectively.

$$d_z = 1 - \frac{1+b_z+c_z}{p_{z1}p_{z2}-(p_{z1}+p_{z2})+1} \quad \cdots\cdots (21)$$
$$e_z = p_{z1}p_{z2}(1-d_z)-c_z \quad \cdots\cdots (22)$$

The "assigned poles" of $\tau = 0.006$ s are at 0.9576 ± 0.055j and 0.9591 ± 0.013j. The zeros are at 0.9911 ± 0.0263j. The complex zeros at lower positions than the poles, creates the oscillatory step response. Therefore, the zeros should be assigned at 0.9576 ± 0.055j to cancel out the poles. Moreover, the parameters, d_z and e_z, are calculated using Eqs. (20) and (21), yielding $d_z = 0.84$ and $e_z = -0.8357$. The step response is indicated by the red curves in Fig. 16, which are smoothened by the feedforward controller. Responses of the gain perturbation of the plant, ±30%, are also indicated by dashed curves and dotted curves in Fig. 16. The feedforward controller does not affect the perturbation of the plant. The graph shows that the effects of the perturbation are the same, irrespective of whether we use the feedforward controller.

6. Conclusion

The control system of the lens actuator of the camera module for smart phones was discussed. First, we simulated the three cases of resonant frequency and zero cross frequency, and confirmed that the system can be stabilized by each controller. Next, the three pole assignment methods were discussed: namely 1) the multiple pole method, 2) CDM, and 3) the optimal controller derived from an algebraic expression. We decided to use CDM because of its fast convergence without oscillation. The limited pole assignment method proposed by the author, is applied to redesign the CDM controller to a digital controller and to confirm both that the response is less oscillatory than the Tustin transform, and that the bound of the stability is determinable. Finally, the feedforward controller is introduced to smoothen the step response. These results confirm that the control system, with a zero cross frequency near the plant resonant frequency, can be controlled with sufficient stability, and moved with sufficient smoothness.

Acknowledgment

I would like to express my deep appreciation to Dr. Manabe, ex-professor at Tokai University, for his valuable comments and suggestions.

References

(1) H. Nakajima and H. Ogawa: "Compact Disk Technology", Chap.6, IOS Press, Washington D.C. (1993)
(2) D. Koide, H. Yanagisawa, H. Tokumaru, H. Okuda, K. Ohishi, and Y. Hayakawa: "Feed-Forward Tracking Servo System for High-Data-Rate Optical Recording", Jpn. J. Appl. Phys., Vol.42, No.2B, pp.939–945 (2003)
(3) E. Yokokawa: "A Servo System to Improve the Playability of Optical Disk Drive", *IEEJ Trans. on IA*, Vol.125, No.3, pp.277–285 (2005) (in Japanese)
(4) Y. Urakawa: "An Application of the Initial Value Compensation Method to a Multi-Rate Controller of Optical Disk Drives", 2009 IEEJ Industry Applications Society Conference, 2-O4-4 (2009) (in Japanese)
(5) S. Manabe: "Brief Tutorial and Survey of Coefficient Diagram Method", The 4th Asian Control Conference, Singapore, pp.1161–1166 (2002)
(6) S. Manabe: "COEFFICIENT DIAGRAM METHOD", 14th IFAC Symposium on Automatic Control in Aerospace, Seoul, pp.211–222 (1998)
(7) L. Qiu and K. Zhou: "Preclassical Tools for Postmodern Control", IEEE Control System Magazine, pp.26–38 (2013)
(8) Y. Urakawa: "Parameter Design for a Digital Control System with Calculation Delay Using a Limited Pole Placement Method", *IEEJ Trans. on IA*, Vol.133, No.3, pp.272–281 (2013) (in Japanese)
(9) Y. Urakawa: "Studies on Limited Pole Placement Method Considering Calculation Delay of Digital Control System", Doctoral Thesis, Yokohama National University (2013) (in Japanese)
(10) A. Takano: "2-Degree-of Freedom Self-Tuning Control for Motor Drives Using Pole-Zero Cancellation Method", *IEEJ Trans. on IA*, Vol.129, No.4, pp.415–422 (2009) (in Japanese)

(11) Y. Urakawa and T. Watanabe: “A Study of High-Gain Servo Controller with Complex Zeros for Optical Disk Drives”, *Jpn. J. Appl. Phys*., Vol.44, No.5B, pp.3427–3431 (2005)
(12) W. Messner, M. Bedillion, L. Xia, and D. Kams: “Lead and lag compensators with complex poles and zeros: design formulas for modeling and loop shaping”, *IEEE Control Systems Magazine*, Vol.27, No.1, pp.44–54 (2007)

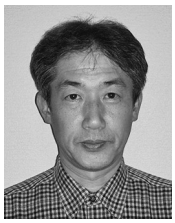

Yoshiyuki Urakawa (Member) received the B.E. degree from the Department of Mathematical Engineering and Information Physics, University of Tokyo, in 1983. He joined Sony in 1983, and works on the signal processing of digital VTR, the research of a parameter design for industrial robotics, and the design of servo system for optical disk drives. He received the D.E. degree from Yokohama National University in 2013. His interests are in motion control and high- performance servo systems.